

UNIVERSIDAD DE LAS AMÉRICAS PUEBLA
Engineering School
Chemical and Food Engineering Department



**A NEW METHOD TO PREDICT JET FLAMES PROPERTIES THROUGH
GEOMETRICAL MODELS**

Scientific Article Presented As Part Of The Requirements For The Graduation In The
Honours Program Of

Adrian de Jesus Jano Fong

156074

Joseph Nahim Ramirez Castelan

159215

Licenciatura in Chemical Engineering

Advisor: Adriana Palacios Rosas, Ph.D.

San Andrés Cholula, Puebla.

Spring 2021

Signature sheet

Scientific Article that to complete the requirements of the Honors Program present the students **Adrian de Jesus Jano Fong, ID: 156074** and **Joseph Nahim Ramirez Castelan, ID: 159215.**

Advisor

Adriana Palacios Rosas, Ph.D.

President

Ricardo Jorge de Albuquerque Martins, Ph.D.

Secretary

René Ledesma Alonso, Ph.D.

2 **A NEW METHOD TO PREDICT JET FLAMES PROPERTIES THROUGH**
3 **GEOMETRICAL MODELS**

4 A. Palacios^{1*}, A. Jano¹, J. Ramirez¹

5 ¹ *Universidad de las Americas Puebla, Departamento de Ingeniería Química, Alimentos y*
6 *Ambiental. Santa Catarina Martir, San Andres Cholula, Puebla. C.P. 72810. Mexico.*

7 **Abstract**

8 The study of jet fire types and nature represents a step forward in the chemical industry safety
9 This article proposes a new method with MATLAB[®] to automatically read jet fire images
10 and obtain the flame properties. Determining values of volume, height, lift off, and width of
11 the flames. Also, the method implements theoretical models for estimating flame volume as
12 geometric ellipsoid, geometric kite, regression model, image processing and a new proposed
13 model by Jano & Ramirez.

14 Furthermore, the results obtained are compared with the data reported by Garcia and Palacios,
15 who analyzed the same flame images by regression model. It was concluded that the proposed
16 method is more precise, efficient, and faster compared to the method used by Garcia and
17 Palacios. The method for jet fires images, achieves an average speed processing of 6.2 images
18 per second, under different conditions of pressure or methane volumetric flow.

19 *Keywords:* Jet fire; flame shape; flame height, automate method; MATLAB[®].

20
21 **Resumen**

22 El estudio de los tipos de *jet fires* y su naturaleza representa un paso adelante para la
23 seguridad en la industria química. Este artículo propone un nuevo método con MATLAB[®]
24 para leer automáticamente imágenes de *jet fire* y obtener propiedades de la llama; volumen,
25 altura, *lift off* y ancho de la llama. Además, el método implementa modelos teóricos para

* *Corresponding author. E-mail: adriana.palacios@udlap.mx*

26 estimar el volumen de la llama como elipsoide geométrico, cometa geométrico, modelo de
27 regresión, procesamiento de imágenes y un nuevo modelo propuesto por Jano & Ramírez.

28 Además, los resultados obtenidos se comparan con los datos reportados por García y
29 Palacios, quienes analizaron las mismas imágenes de llama mediante modelos de regresión,
30 lo que llevó a la conclusión de que el método propuesto es más preciso, eficiente y rápido en
31 comparación con los métodos utilizados por García. y Palacios. Este método para imágenes
32 de *jet fires* logra una velocidad promedio de procesamiento de 6.2 imágenes por segundo,
33 bajo diferentes condiciones de presión o flujo volumétrico de metano.

34 *Palabras clave:* Dardos de fuego, forma de flama, altura de flama, metodología automática,
35 MATLAB®.

36

37 **1. Introduction**

38 Accidents in the Chemical Industry have resulted in substantial economic losses,
39 environmental damage, and human casualties (Casal, 2017). Therefore, the safe production,
40 storage and distribution of chemical products is of utmost importance and the center of a
41 large body of research (Casal, 2017).

42 An industrial accident could be caused by different circumstances, but fire accidents have
43 proved to be an important factor in increasing the impact of the accidents due to the domino
44 effect associated with fire accidents, such as BLEVE (Boling Liquid Expanding Vapor
45 Explosion). One example of the dangerous combination of Jet fires and BLEVE is the
46 accident of San Juanico, where approximately 500 human lives were lost (Hemmatian *et al*,
47 2015). Consequently, several actions and systems have been developed and implemented in
48 order to improve fire safety (Casal, 2017).

49 Examples of efforts are the DOW'S Fire & Explosion Index Hazard Classification Guide and
50 the SFPE Handbook of fire Protection Engineering (AIChE, 2016; Hurley *et al*, 2015), which
51 are valuable safety references. Both references analyze key factors like material factors,
52 economic values (AIChE, 1994), the reliability and computer simulations (Hurley *et al*, 2015)
53 in order to prevent accidents and domino effects in chemical industries.

54 Jet fires property analysis history dates to 1948, with the first studies of flame length (Hottel,
55 & Hawthorne, 1948) and diffusion flames (Wohl, & Gazley, 1948). Later, in 1978, it was
56 assumed that unstable flame analyses were senseless due to the unsteady flame state over
57 time (Annushkin & Sverdlov, 1978), therefore, the focus changed to the analyses of stable
58 flames and visible flame length in vertical jet flames diffusion (Becker, & Liang, 1978). By
59 1984, the concepts of lift-off heights and visible vertical turbulent jet diffusion flames lengths
60 were formally introduced in the literature (Kalaghatigi, 1984) and different solution methods
61 were explored.

62 The fire computer simulation methods aim to analyze possible fire scenarios to obtain fire
63 property data; nevertheless, the mathematical models and computational power to analyze all
64 the fire scenarios have been limited, therefore, different approaches and models can be
65 explored in order to predict fire property data (McDermott *et al.*, 2008). In this context,
66 authors have proposed some geometrical models to characterize the flame and stated how
67 flame properties data could be calculated. Some examples of geometrical models include:
68 the ellipsoid (Baron, 1954), the cylindrical ascendent disks (Orloff, 1981), the cone
69 (Chamberlain, 1987), the rectangle (Palacios, A. 2011) and the kite (Zhou, 2016).

70 Flame properties can be also analyzed from mathematical approach, through regression
71 analysis as it is proposed by Palacios *et al* (2017) and further explored by Garcia (2019).
72 Nevertheless, the flame properties data obtained by this method consumes a considerable
73 amount of time, as in both references, the estimated time was almost three years.

74 Moreover, computer simulation and flame modelling depend on the physics characteristics
75 of the flame such as lift off, width, height, and area, but the volume depends on the model
76 use to measure it (geometric or mathematical) that is being consider for its calculations

77 In this work, an efficient and optimized computational method using a MATLAB[®] code is
78 proposed, as part of a new method for the flame properties calculus. The MATLAB[®] code
79 can analyze and compute some of the physical flames properties and the flame volume
80 considering four models: Zhang (2015a), Orloff (1981), Zhou (2016), and Jano & Ramirez
81 (2021).

82 The present work analyzes 8 methane flame conditions, classified into two groups (P flames
83 and V flames) of four flame conditions. The P flames were obtained from a constant
84 volumetric flow of 10.24 L/min, at 0.7, 0.8, 0.9 and 1 atm. The P flames have been previously
85 tested and evaluated by Garcia (2019). The V flames were obtained at constant pressure of 1
86 atm, at volumetric flows of 7, 8, 9 and 10 L/min). V flames have been also analyzed, by
87 Palacios *et al* (2017).

88 The experiments carried out in the present study were obtained from a collaborative research
89 work between UDLAP and University of Science and Technology of China (USTC),
90 financially supported by the Royal Society, UK (UDLAP *et al*, 2014).

91 **2. Experimental design**

92 Experimental methane jet fires were carried out in the Laboratory of Fire Science and
93 Technology of the USTC. Figure 1 depicts an outline of the experimental set-up, consisting
94 of a flow supply system, with a 2 m long pipe, a stainless-steel nozzle, and a low air pressure
95 chamber of 3 m (width) x 2 m (length) x 2 m (height). The ambient pressure inside the
96 chamber was regulated and maintained by a vacuum pump and controlled by a pressure
97 sensor. As the ambient pressure decreased, other parameters affecting the jet fires
98 development also decreased: the amount of oxygen per unit volume, the fuel the mass flow
99 rate of the gas released through the orifice. Each test began when the pressure inside the
100 sealed chamber was stable for a period of about 5 min after pumping fresh air into the low-
101 pressure chamber to replace previous air. The duration of each experimental test was 2 min.

102 Table 1. Experimental conditions of the partially premixed methane-air jet flames.

Fuel (L/min)	Air (L/min)	Air supplied (%)
7	0-2.92	0-29
8	0-2.9	0-27
9	0-3	0-25
10.24	0-3.2	0-24

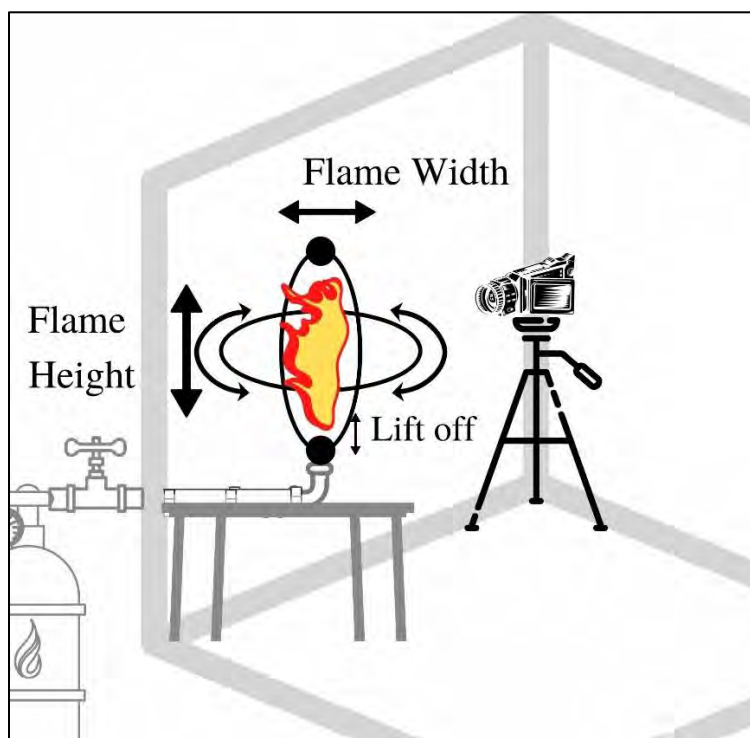
103

104 During all the tests, the following parameters remained constant: an ambient temperature of
105 25 °C, a relative humidity of 35%, and a nozzle diameter of 3 mm. Through a flow rate meter,
106 the fuel supply rates and hence fuel jet exit velocities at the nozzle were controlled.

107 For the P flames, it was obtained the geometrical characteristics of the vertical subsonic
108 flames at normal and sub-atmospheric pressures of 1.0, 0.9, 0.8, & 0.7 atm at constant
109 volumetric methane flow rate of $\dot{V}_{or} = 1.71 \cdot 10^{-4} \text{ m}^3/\text{s}$. For the second set, V flames, it
110 was under the same conditions, just varying the volumetric methane flow rate to 7, 8, 9 and
111 10 L/min at constant atmospheric pressure $P = 1$ atm.

112 A charged-coupled device (CCD) digital camera of sensor size 8.5 mm and an image size of
113 320 x 240 pixels was used to film the jet fire experiments. Each methane flame condition had
114 an average of 750 images captured.

115



116

117 Figure 1: Representative Set-Up diagram of the experiments conducted at the labs of the University of
118 Science and Technology of China. (Jano & Ramirez, 2021)

119

120

121 **3. Methodology**

122 This work methodology is divided in two main ideas. The first part points out the general
123 process of the computational method used to read and calculate the jet fires properties,
124 explaining how it was implemented and the flame properties obtained. The second part
125 describes the models used for the flame volume estimations.

126 *3.1 Flame image processing method*

127 The method proposed in this work aimed to read and process images of any fuel jet fires
128 recorded. The main idea is to achieve a fast and precise obtention of the flame properties, to
129 calculate the volume of the flame with different models. All the mentioned above with the
130 intention of automatize the study of jet fires and their properties.

131 *3.1.1 Properties obtention*

132 Flame images are load as a database into MATLAB[®] and the image type of the flame is
133 specified. These images undergo a process of qualification, in which the spectrum of the
134 flame is split into red, green, and blue masks. The green mask is filtered, since flames mostly
135 round in the blue and yellow colors, the wavelength of blue color is around 450 nm and for
136 yellow color is 550 nm. According to Shefer *et al* (2009) and Frank *et al* (2000) the jet fire
137 electromagnetic spectrum is mostly presented between 375 to 540 nm. And more specific,
138 the laminar flow of methane combustion spectrum, according to the work of Shefer (2009)
139 lies between 410 and 450 nm, which can be appreciated in the blue flame, Figure 2.

140 The binarization of the image is performed accordingly with the intensity of the flame. Due
141 to the refraction of the photons at the time of capturing the flame images, the brightness of
142 the frames constantly varies. That is why the code automatically calibrates the intensity of
143 the flame with an adaptive threshold, allowing a smooth reading of the flame structure in the
144 frames.

145 After the color selectivity, the clearing of the shape is done by homogenizing the interior of
146 the flame, as it is shown in Figure 2. The binarization process is performed in a custom
147 cropped image to increase the clarity of the flame and avoid the misread of some highlights

148 or flashes outside the flame due to the reflex that the flame causes. Figure 2 shows a process
149 of reading, binarize and clear the image of a flame.

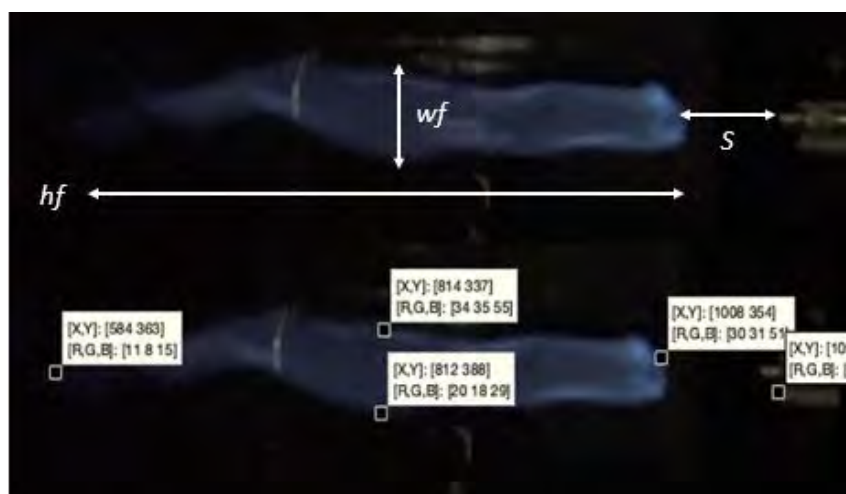


150

151

Figure 2: Image binarization process. (Jano & Ramirez, 2021)

152 Once there is a clear image of the flame, Figure 3, the pixel coordinates of the flame are used
153 in order to obtain the following flame properties in pixels: the height (h_f) width (w_f), lift off
154 (s) and vertical area (A_f), for more detail see Annex B. The data provided by these flame
155 properties in pixels is used to calculate the flame volume for the four different geometric
156 models accordingly with each model equation.



157

158

Figure 3: Pixel properties obtention. (Jano & Ramirez, 2021)

159 It must be clarified that at this point, the flame properties are expressed as pixels, therefore a
160 pixel-meter ratio (P2M) was used. The P2M is a conversion factor from pixel to meters that
161 was used for this method and is strictly related to the experiment dimensions used in the

162 laboratory. The P2M value change between P flames and V flames because the camera angle
163 between each experimentation was changed, leading to a P2M values of 800 [pixel/meter]
164 for P flames and 700 [pixel/meter] for V flames. For more details on the calculation of the
165 P2M see Annex A.

166 After obtaining the flame properties required (h_f, w_f, A_f, s) the program calculates the flame
167 volumes by Zhang (2015a) model ($V_{f, ellipse}$), Orloff (1981) model ($V_{f, Orloff}$), Zhou (2016) model
168 ($V_{f, kite}$) and the proposed circular base model (V_f) (Jano & Ramirez, 2021). These models are
169 explained with more detail in section 3.2.

170 The results obtained in MATLAB[®] are stored in a Microsoft Excel[®] file, to calculate the
171 average values for: lift off; flame height; flame width; and the flame volumes for the four
172 different geometric models considered. All the previous calculus is done for each methane
173 flame condition. Likewise, it is calculated a flame lecture stability (f_s) for the jet fires.

174 The flame lecture stability is a proposed property that measures the flame lecture regularity
175 of the method along each methane flame condition. It uses the average volume of the methane
176 flame condition and compares it against each image (k), evaluating from 0 to n , where n is
177 the last image, Eq. (1). Then an average flame lecture stability is obtained by applying an
178 average theorem in all the results of Eq. (1).

179
$$f_s = \overline{\left(\frac{V_k - \bar{V}}{\bar{V}}\right)}, k | 0^n \quad (1)$$

180 At higher flame lecture stability values, then the lecture of the jet flame may be classified as
181 irregular, but at lower flame lecture stability values, the jet flame lecture of the method can
182 be classified as stable.

183 *3.2 Flame properties models*

184 Several models have been proposed to estimate flames properties such as height, lift off,
185 width, and volume. Geometric figures have been proposed, such as, prolate spheroid by
186 Zhang (2015a) based on the ellipse of Baron (1945), or kite geometry by Zhou (2016).
187 Likewise, there are mathematical models proposed, such as Garcia's regression model
188 (2019), which suggests the calculation of the flame volume using a polynomial formula.

189 Other research used film images and proposed methods to compute flame properties, such as
190 the cylindrical disks from Orloff (1981). This research follows the last approach proposing a
191 method based on MATLAB[®] code to analyze binary images.

192 Even though, there are many other important different models to predict jet flames properties,
193 most of them are more focused on the thermal radiation than the geometry. For example,
194 Palacios *et al* (2012) proposed a solid flame model, which describes the flame radiation
195 emission as a frustum cone. Lowesmith (2007) proposed a one-point radiation model. Ekoto
196 (2014) described a multipoint source radiation model. And Zhou (2015) a line source
197 radiation model, later integrated with the Kite model (Zhou, 2016).

198 For this study, the aim is to compare visual properties as volume, and the other properties
199 already mentioned. The experimental results did not include thermal radiation data; thus, the
200 radiation models were not considered. However, according to Zhou (2015), the kite model
201 describes better the radiation emittance, and is the one used for the Kite model (Zhou, 2016).
202 Hence, kite's model is the only one which was considered from all the radiation models
203 mentioned.

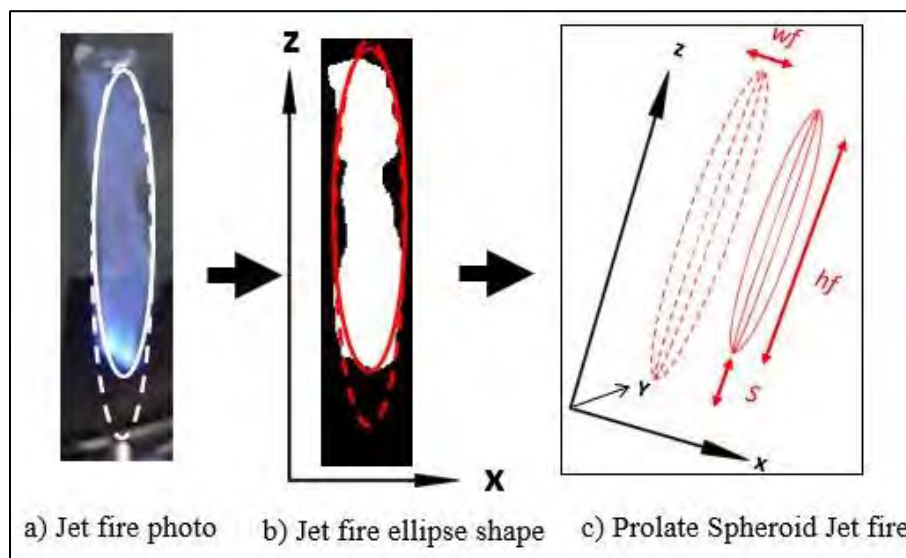
204 3.2.1 Geometric volume approach

205 In the case of geometric models, the objective is to adapt the geometric figure to the flame to
206 calculate a flame volume. Therefore, different geometrical figures have been proposed
207 (Section 3). For the purpose of this article, the geometric figures of a Kite (Zhou, 2016) an
208 ellipsoid (Baron, 1954; Zhang, 2015a) and the circular base model proposed (Jano &
209 Ramirez, 2021) were considered, calculated, and compared. The reason why these geometries
210 were considered is because they have shown accuracy to predict thermal radiation in different
211 works (Zhou, 2016) (Zhang, 2015a).

212 3.2.1.1 Ellipsoid Geometry

213 Baron's (1954) jet fire figure proposed an ellipse form using the height of the flame (h_f).
214 Based on this geometry, Zhang *et al* (2015a) proposed a mathematical model to obtain the
215 flame volume, using h_f as geometrical parameter, to study the combustion characteristics
216 during gaseous fuels energy conversions. The experimentation consisted in turbulent gaseous

217 propane jet flames produced by different diameter nozzles at 64 kPa, which lead to two types
 218 of ellipse analyses (Figure 4).



219

220 Figure 4: Baron (1954) ellipse and Zhang (2015a) prolate spheroid volume estimation. The dotted line
 221 considers the lift off (s) and the solid line does not. (Jano & Ramirez, 2021)

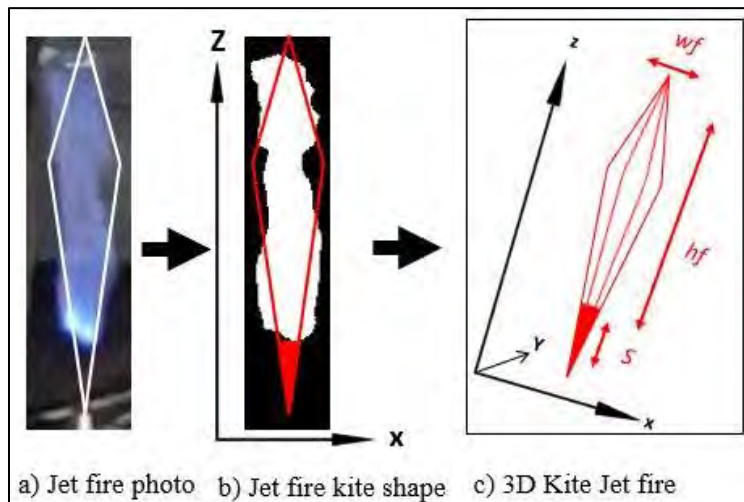
222 Consequently, Eq. (3) is proposed to estimate the volume of the flame, in which b is a
 223 constant that depends on the fluid pressure. According to Baron (1954), for flows at normal
 224 pressure, b must be equal 0.29, and for sub-atmospheric flows b must be equal to 0.2.

225

$$V_{f,ellipse} = \begin{cases} \frac{\pi}{36} b^2 h_f^2 & s = 0 \\ \frac{\pi}{36} b^2 h_f^2 + \frac{\pi}{12} b^2 h_f^2 s + \frac{\pi}{12} b^2 h_f s^2 - \frac{\pi}{12} b^2 s^2 \ln\left(\frac{h_f+s}{s}\right) & s > 0 \end{cases} \quad (2)$$

226 3.2.1.2 Kite Geometry

227 Zhou *et al* (2016) explained that the heat transfer of the jet fire is adjusted to a kite (Figure
 228 5) experimenting with vertical and horizontal propane flames of up to 5 m length with
 229 different flow rates between 390 kg/h and 100 kg/h, and a release pressure of 7.5 atm. This
 230 geometry considers most of the flame shape, Figure 5, meaning that the calculus of volume
 231 estimation significantly contemplates the full real flame volume. Also, the model from Zhou
 232 *et al* (2016) acknowledges the lift off and discriminates the volume below it.



233

234

Figure 5: Zhou (2016) kite volume estimation. (Jano & Ramirez, 2021)

235 Remarkably, Zhou *et al* (2016) compared radiation predictions from different flame shapes
 236 models (Lowesmith 2007; Ekoto 2014; & Palacios 2012) and furthermore, proposed a
 237 thermal model based on a kite jet flame shape. Therefore, Zhou *et al.* (2016) does not
 238 calculate the flame volume directly. Hence, to integrate Zhou *et al.* (2016) model for
 239 comparison purposes in this work, Eq. (3) was developed to represent the volume obtained
 240 (Figure 5c), as suggested by Zhou *et al* (2016).

241

$$V_{f,kite} = \left[\frac{(w_f^2 * (h_f + s))}{3} \right] - \frac{\left(\frac{w_f * s}{2(\alpha h_f + s)} \right)^2 * s}{3} \quad (3)$$

242 Despite looking like a geometry that could not predict better the jet fire than the Baron's
 243 ellipse (1954), the work of Zhou *et al* (2016) demonstrated that the kite geometry predicts
 244 more accurately the thermal radiation. Nevertheless, both geometries are included in the
 245 comparison.

246 3.2.1.3 Circular Base Proposed Model

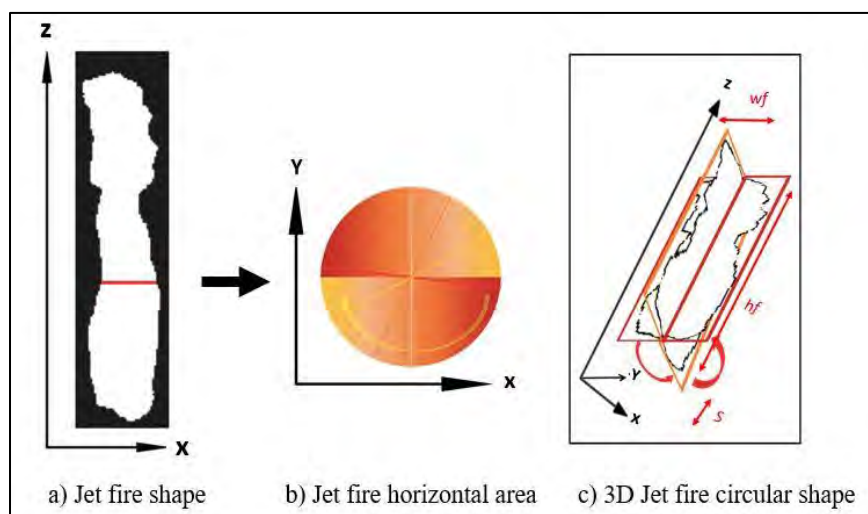
247 It is proposed to use the real vertical area x-z axis (A_f) of the jet fire obtained by the computer
 248 and MATLAB[®], and estimate the volume from it, rotating the area and obtaining a more
 249 precise volume without limitations imposed by fixed geometries (Figure 7). The model
 250 assumes that the base on the x-y axis is circular (Figure 7b). The main reason of that
 251 assumption is because the geometry of a sphere has been studied and accepted for jet fires
 252 by several researchers. Dietrich *et al* (1995), and Zhang *et al* (2015b) worked with

253 microgravity combustion, obtaining a spherical shape for the flame at microgravity
 254 atmospheres. Sunderland *et al* (1999), Dietrich *et al* (2000), and Кузнецов *et al* (2020)
 255 studied laminar jets at non buoyancy atmospheres, getting spherical geometries as well. In
 256 Figure 6 it can be more appreciated the shape described.



257
 258

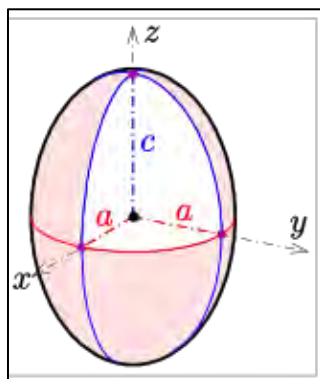
Figure 6: Laminar jet fire of C_2H_4 at microgravity conditions. (Zhang *et al*, 2015b)



259
 260

Figure 7: Circular base proposed model. (Jano & Ramirez, 2021)

261 The flame volume was calculated adapting the theoretical volume of a prolate spheroid,
 262 Figure 8.



263
 264

Figure 8: Theoretical volume of prolate spheroid. (Ag2gaeh, 2015)

265 Eq. (4) was used to obtain the vertical area of the prolate spheroid (x-z axis), and Eq. (5) for
266 the volume of the prolate spheroid. (Zwillinger, 2011):

$$267 \quad A_e = \pi * a_e * c_e \quad (4)$$

$$268 \quad V_e = \frac{4}{3} * \pi * a_e^2 * c_e \quad (5)$$

269 The main idea of the model is to calculate a volume (V_e) from the vertical area (A_e).

$$270 \quad V_e = \frac{4}{3} * a_e * A_e \quad (6)$$

271 Finally, the volume was modelled in terms of the area $V(A)$, using Eq. (4) and (5), Eq. (6)
272 was obtained. In terms of the jet fire, the radio on the z axis (c_e) represents the half of the
273 height of the flame (h_f) then $c_e = h_f/2$. The width of the fire is represented by twice the radio
274 on the x axis $2a_e = w_f$. And the vertical area (A_e) represents the vertical area of the jet fire,
275 obtained by the computer $A_e = A_f$. Then it is obtained Eq. (7), representing Figure 7c.

$$276 \quad V_f = \frac{2}{3} * w_f * A_f \quad (7)$$

277 3.2.2 Mathematical volume approach

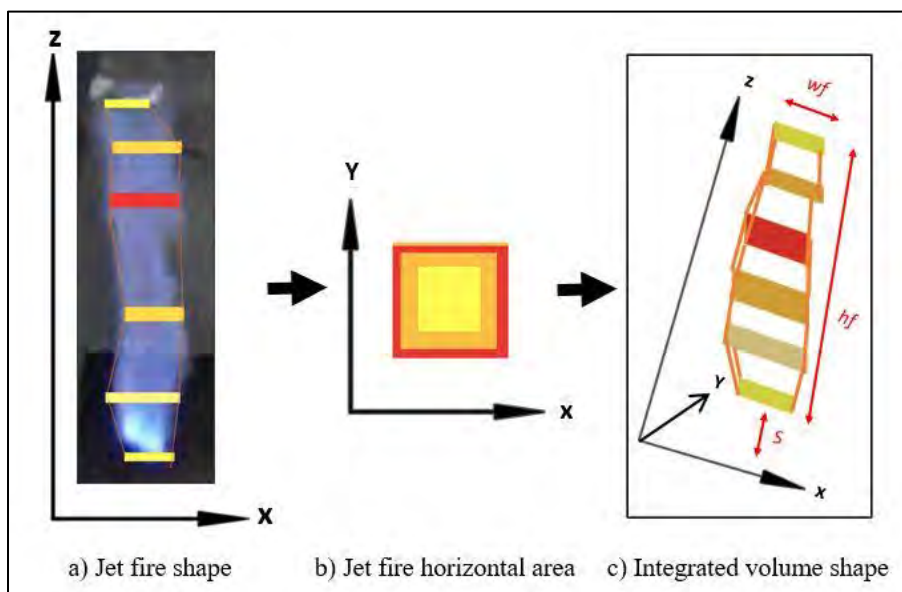
278 The flame volume of a jet fire can also be estimated using a mathematical approach (Palacios,
279 2017; Garcia, 2019). These methods do not correlate the volume to a specific geometric
280 shape, instead, try to describe the flame volume with a mathematical behavior. To add these
281 mathematical methods to the comparison, the models of Garcia (2019) and Palacios (2017)
282 have been included.

283 3.1.2.1 Regression Model

284 Palacios (2017), and later Garcia (2019), proposed a method on flame images using Paint®
285 and Microsoft Excel® to define the lift off, the height of the flame, and 10 diameters of the
286 flame, each at every 10% of the height along the z axis, Figure 9a. The objective was to
287 establish a relation, between the flame and a regression model, to calculate the flame volume.

288 After manually obtaining the properties (h_f , w_f , s), the diameters were used to develop a
289 regression equation that calculated the flame volume. Garcia (2019) and Palacios (2017)

290 assumed a square perimeter, Figure 9b, to calculate an area for each measured diameter,
291 Figure 9a. Then, the areas were tabulated in Excel[®] to obtain a behavior expressed in a
292 polynomial function. Finally, the polynomial function was integrated along the flame height
293 to obtain the volume of the flame (Figure 9).



294

295 Figure 9: Regression model used by Garcia (2019) and Palacios (2017). (Jano & Ramirez, 2021)

296 3.2.3 Flames image properties obtention

297 Orloff (1981) was the first to conceive the use of use image processing to study fire properties
298 but lacked the tools to do it efficiently. Nowadays, image processing effectively implemented
299 in the study of jet fires is already possible (e.g., Garcia, 2019; Shen *et al*, 2017).

300 3.2.3.1 Cylindrical ascendent disks (Orloff)

301 In 1981, Orloff proposed a method to obtain the volume of the flame from a two-dimension
302 image (x-z axis), arguing that the flame can be conceived as stacked disks. Hence, the volume
303 of the flame can be calculated by integrating the volume of the stacked disks (defined by the
304 product of the horizontal length and circular area x-y axis, Figure 10).

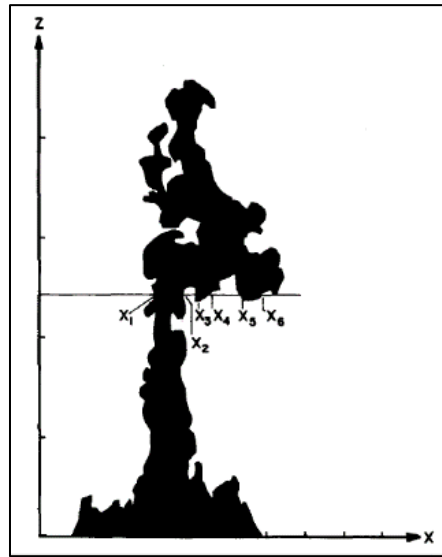


Figure 10: Orloff model image processing. (Orloff, 1981)

305

306

307 4. Results and Discussions

308 All the images of the 8 methane flame conditions (P and V flames) were analysed by the
 309 proposed method, obtaining results for each volume estimation model. Average flame
 310 volume results are compared graphically. Furthermore, results are compared against Garcia
 311 (P flames) and Palacios (V flames) results, in order to analyse the proposed method flame
 312 lecture accuracy and contrast the image processing speed of Palacios and Garcia's method
 313 against the proposed method.

314 4.1 Analysis of flame properties from proposed method

315 4.1.1 Vertical subsonic methane jet flames at constant volumetric flow (10.24 L/min) at 316 different pressures (P flames).

317 The flame volume behaviour patterns, obtained by Garcia method and the proposed method,
 318 are that at sub-atmospheric pressure if there is less pressure then the greater the volume is,
 319 nonetheless the flame volume at atmospheric conditions has a bigger volume than the 0.8
 320 atm and 0.9 atm volume but it is smaller compared to the 0.7 atm flame volume (Figure 10).

321

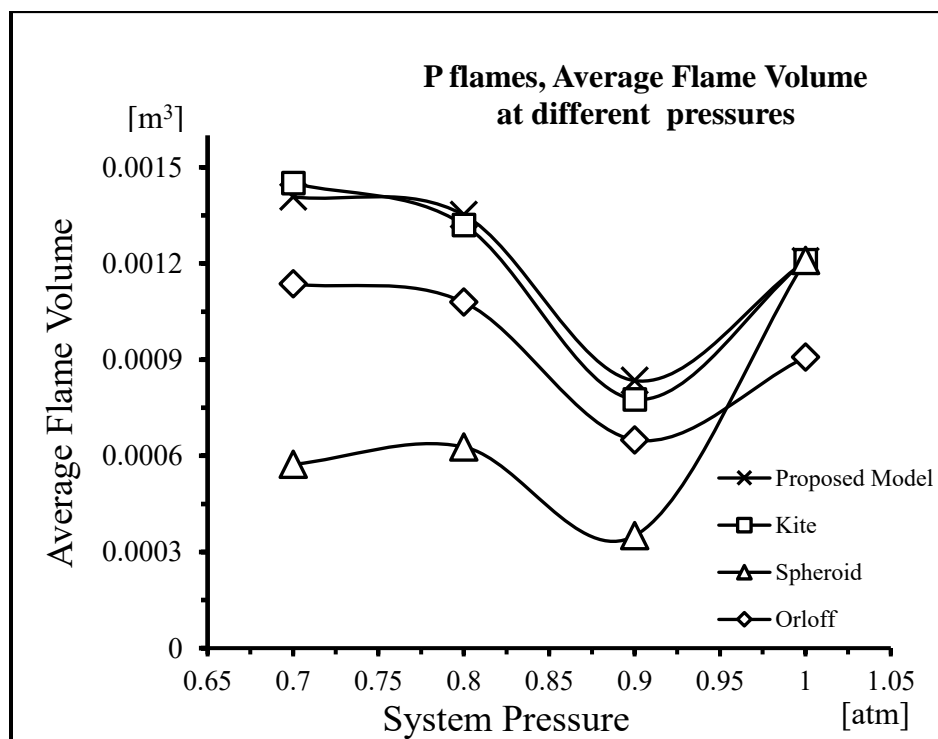


Figure 10: P flames Average Flame Volume at 10.24 L/min. (Jano & Ramirez, 2021)

322
323

324 Regarding the comparison with the results from Garcia (2019), it is determined that in 0.7
325 atm and 0.8 atm the flame volume results are very similar with the proposed model and the
326 Kite geometric model. Also, the behaviours of Garcia's results are the same as the one
327 obtained in the proposed method. Despite existing a difference in the results at 0.9 atm, it
328 could be explained due to the main differences in the flame volume estimation. (Figure 10).

329 4.1.1.1 Flame Lift off

330 The flame lift off behaviour pattern of P flames can be observed in Figure 11a, at a lower
331 pressure the biggest lift off is obtained. Nonetheless, the lift off behaviour pattern reported
332 in Garcia (2019) is similar to the behaviour pattern obtained by the proposed method,
333 meaning that there exists a proper flame lecture in the proposed method, as a matter of fact,
334 the values of 0.9 atm and 1 atm are very much similar, 0.049 m and 0 m respectively.

335 4.1.1.2 Flame width

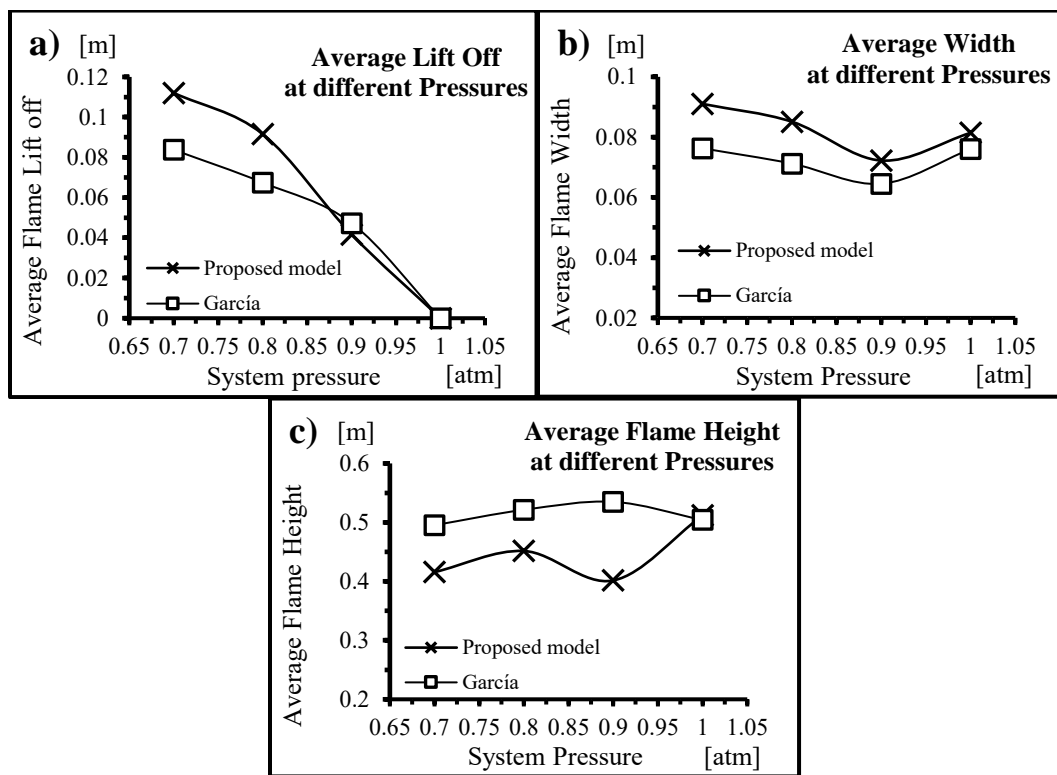
336 The flame width behaviour pattern is analogous to the pattern of volume, Figure 11b. The
337 width values of Garcia (2019) and the calculated in the proposed method have the same
338 behaviour pattern, however, the range results do not coincide. The discrepancy in the proper
339 values could be occasioned because of the use of a different P2M, or the accuracy on the

340 measure of the program against the manual obtention used by Garcia. Anyhow, the closeness
 341 on the results is high, just differing 1 mm at most.

342 4.1.1.3 Flame height

343 The flame height behaviour calculated with the proposed method shows an increasing and
 344 decreasing pattern, because the 0.7 atm and the 0.9 atm flame height are smaller than the 0.8
 345 atm flame height, but 0.8 atm has a smaller flame height than at 1 atm, Figure 11c. On the
 346 other hand, Garcia (2019) flame height behaviour pattern increases at sub atmospheric
 347 pressure near the atmospheric pressure, but once the flame reaches the atmospheric pressure
 348 the flame height decreases a little. discussion

349



350

351 Figure 11: Constant Volumetric Flow 10.24 L/min at different Pressure comparison. a) Average Flame Lift
 352 off, b) Average Flame Width, c) Average Flame Height. (Jano & Ramirez, 2021)

353 4.1.1.4 Flame lecture stability

354 The flame lecture stability of the P flames volume values from Garcia method and the
 355 proposed method are shown in Table 2. The average flame lecture stability of all the data is
 356 17.22%, the highest is at 0.9 atm from the Garcia Regression model and the lowest is
 357 10.83% at 1 atm from the Orloff (1981) model, meaning that there exists a small unsteady

358 methane flame along in the time, but a general behaviour pattern can be pointed out, which
 359 allow us to understand the methane flame behaviour at the specified conditions.

360 Table 2. Flame lecture stability. Constant Volumetric flow (10.24 L/min) at different Atmospheric Pressure
 361 (0.7, 0.8, 0.9, 1 atm).

Data	Pressure [atm]	Proposed Model	Kite (Zhou)	Ellipsoid (Baron)	(Orloff)	Regression Model (Garcia)
Flame lecture stability	0.7	14%	20%	19%	11%	16%
	0.8	15%	20%	21%	14%	16%
	0.9	16%	21%	23%	14%	23%
	1	12%	18%	22%	11%	19%

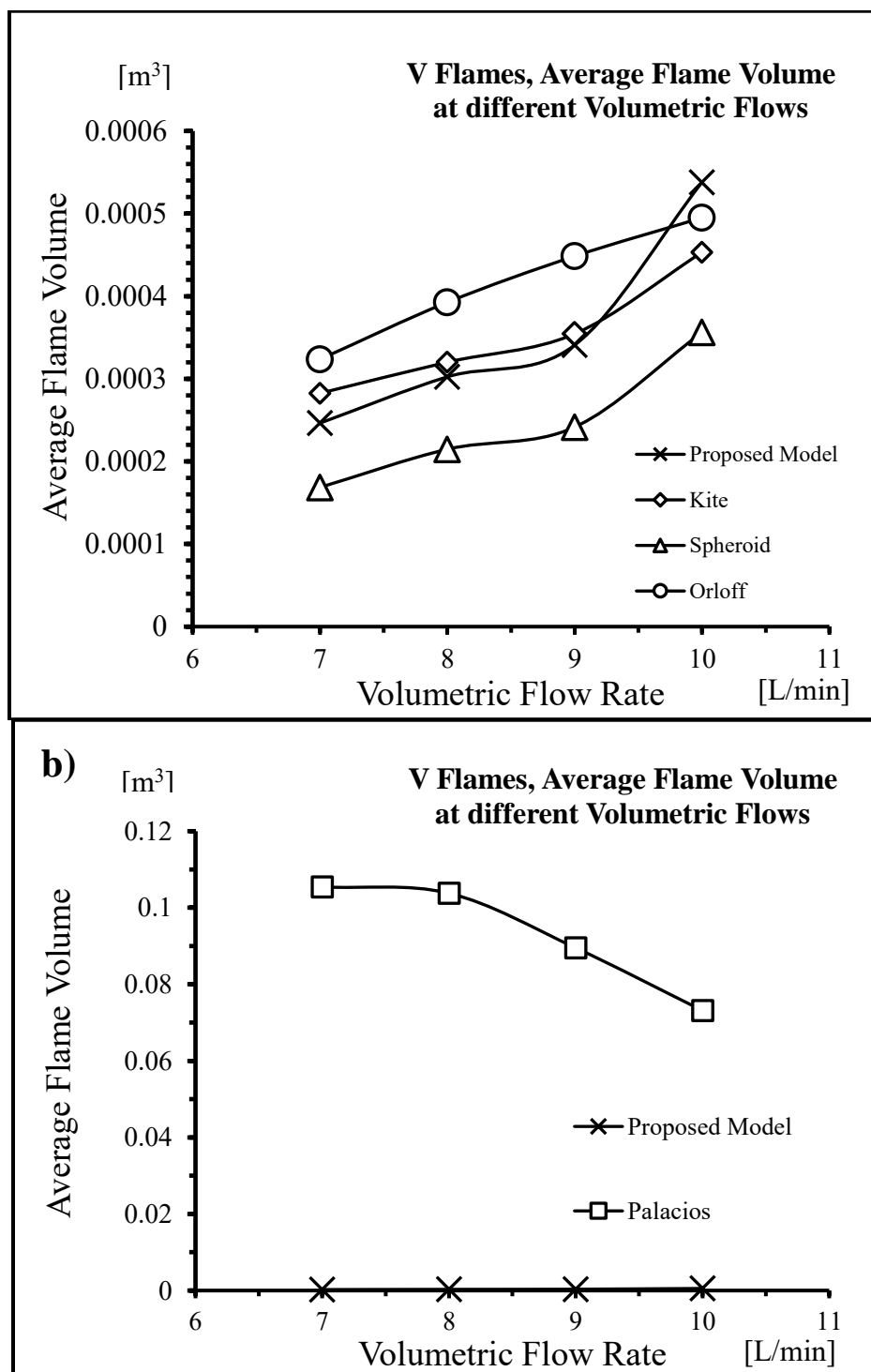
362
 363 The P flame volume reported in Garcia and the one obtained by the proposed method have
 364 similar results. Furthermore, Zhang *et al* (2015a) reported propane flame volume values, at
 365 100kPa and 64 kPa and volumetric flow of 0.01 m³/h (1.666 L/min), are between 0.0012 m³
 366 and 0.0066 m³, in which the maximum volume values are at 100kPa and the lower values are
 367 at 64kPa, giving an average flame volume around 0.003 m³, meaning that P flames volumes
 368 are inside the volume range of literature data for sub-atmospheric pressure.

369 *4.1.2 Vertical subsonic methane jet flames at constant atmospheric pressure at different*
 370 *volumetric flow (V flames).*

371 The V flames average volume obtained by the proposed method, states an increasing
 372 behaviour pattern along with the volumetric flow, Figure 12a, meaning that at constant
 373 pressure, the methane flame volume will increment if the volumetric flow increases. The
 374 increasing behaviour is relatively constant for the Kite, Ellipsoid and Orloff model but the
 375 proposed model had a significant increment from 9L/min to 10L/min. The reason of this is
 376 that the proposed model depends on the flame width in order to calculate its volume and at
 377 these conditions, the average width value is greater than the increasing average flame width,
 378 occasioning that the circular base proposed model could be over-sizing the flame at this point.

379
 380 On the other hand, the average flame volume results from Palacios's method stated a
 381 decreasing pattern and that the average flame volume is much bigger than the one calculated

382 with the proposed method, Figure 12b. This volume difference could be explained by a
 383 different set of factors, which will be discussed later (section 4.1.2.5).
 384



385

386
 387
 388

Figure 12: Average Flame Volume at atmospheric pressure at different Volumetric Flows (7, 8, 9, 10 L/min) comparison. a) Literature models b) Palacios model. (Jano & Ramirez, 2021)

389

390

391 4.1.2.1 Flame Lift off

392 The flame lift off behaviour pattern calculated with the proposed method (Figure 13a), states
393 that the lift off of 8 L/min is smaller than the 7 L/min, but there is an increasing lift-off pattern
394 from 8 L/min to 10 L/min. Differently, from the lift off results by Palacios (2017), it could
395 be observed that the increasing pattern started at 9 L/min. Figure 13a graphically shows that
396 the data calculated from Palacios and the proposed method have a different range of values.
397 While Palacios lift off values are between 0.04 m and 0.065 m, the proposed method lift off
398 values are in a 0.055 m to 0.065 m range. However, the lift off value at 10 L/min is practically
399 0.65 m in both analyses.

400 4.1.2.2 Flame width

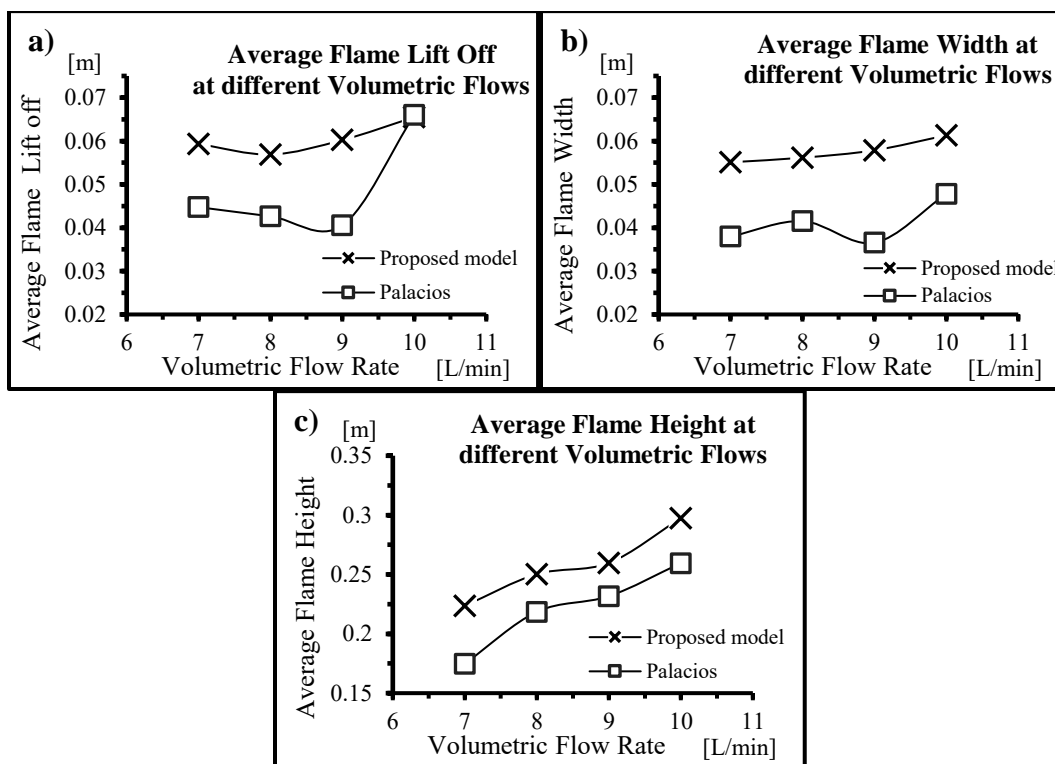
401 The flame width behaviour pattern obtained by the proposed method suggest that the width
402 of the flame should increase along with the volumetric flow, this pattern behaviour can be
403 seen in Figure 13b, but in Palacios's analysis exists an irregularity at 9 L/min that does not
404 fit the increasing width pattern observed in the proposed method results. Moreover, the width
405 values range are slightly different, for Palacios values the range is between 0.036 m to 0.047
406 m, while the proposed method width range is from 0.055 m to 0.062 m

407 4.1.2.3 Flame height

408 The flame height behaviour pattern observed from the values of the proposed method is an
409 increasing pattern which also agrees with the values reported in Palacios's method (Figure
410 13c), as a matter of fact, the results are similar with each other, which means that at a higher
411 volumetric flow a higher flame height will be obtain if the pressure remains constant.

412

413



414

415

Figures 13: Average Flame Height at atmospheric pressure at different Volumetric Flows (7, 8, 9, 10 L/min)

416

comparison. a) Average Flame Lift off, b) Average Flame Width, c) Average Flame Height. (Jano & Ramirez,

417

2021)

418 4.1.2.4 Flame lecture stability

419 The flame lecture stability results of the image processing, which are reported in Table 3,

420 states an average flame lecture stability of 12.36%, in which the maximum value is 22.43%

421 at 7 L/min from the Ellipsoid geometric model and the minimum value is 8.24% at 7 L/min

422 from Orloff's approach but the flame lecture stability of Palacios's method is 75.35%, in

423 which the maximum value is 81.12% at 10 L/min and the minimum is 72.10% at 7 L/min.

424 These results can be explained due to two scenarios: the methane flame is very irregular at

425 every system evaluation or there exists some irregularities in the methane flame property data

426 calculations.

427 Consequently, from the flame lecture stability values of the proposed method and the

428 methane flame videos can be stated that the methane flames behaviour pattern is not that

429 irregular, therefore, the expected flame lecture stability should not have high values. Palacios

430 (2017) method converts some negative flame volume values in positive by applying the

431 absolute value, thus affecting the flame volume calculations which affects the flame lecture

432 stability values.

433

434
435

Table 3 . Flame lecture stability. Constant Atmospheric Pressure (1 atm) at different Volumetric flow (7, 8, 9, 10 L/min)

Data	Vol. Flow [L/min]	Proposed Model	Kite (Zhou)	Ellipsoid (Baron)	(Orloff)	Regression Model (Palacios)
f_s	7	9%	11%	22%	8%	72%
	8	9%	10%	17%	9%	74%
	9	9%	10%	15%	9%	74%
	10	12%	15%	21%	11%	81%

436

437 4.1.2.5 Volume inconsistency at V flames discussion

438 There are three important factors to consider for explaining the volume difference between
439 Palacios's method and the proposed method, the flame lecture stability, the P2M parameter,
440 and the absolute values of the volume obtained in Palacios's method.

441 The flame properties lecture (in pixels) in Palacio's method and the one proposed are quite
442 similar, as it is shown in Table 4. Even though some of the properties slightly differ, the
443 tendency of the properties is similar in both methods, that is why the flame lecture stability
444 is not consider a critical factor explaining the volume differences.

445

Table 4. V flame properties values obtained by Palacios and proposed method.

	Method	Height (pixel)	Lift off (pixel)	Width (pixel)
7 L/min	Palacios (2017)	154.4	39.5	27.9
	Proposed	156.5	41.5	32.7
8 L/min	Palacios (2017)	193.1	37.7	30.5
	Proposed	175.2	39.8	36.7
9 L/min	Palacios (2017)	204.6	35.8	26.9
	Proposed	181.8	42.2	39.2
10 L/min	Palacios (2017)	229.3	59.6	35.2

446

447

448

449 Since the camera vision angle change from P flames to V flames, a new P2M parameter must
450 be calculated, Palacios P2M value used was 883.5 [pixel/metro] and for the proposed method
451 the P2M value is 700 [pixel/metro]. However, both values are similar, which means that the
452 P2M parameter is not a critical factor.

453 Therefore, the final factor is how the volume is calculated. In the regression equations
454 calculated by Palacios (2017), several negative values were obtained and convert into
455 positive values by using an absolute value, which can significantly impact the average flame
456 volume of the methane flame condition. On the other hand, as it was previously established,
457 the P volume values veracity is between literature volume data range, according to Garcia
458 (2019) and the reported values by Zhang *et al* (2015a). Considering the fact that both, P and
459 V flames, are analysed by the same method, it can be assumed that the V flames volumes
460 have certain veracity.

461 On the other hand, in the experimental room at the Laboratory of Fire Science and
462 Technology of USTC behind the flame, there was an unknown material that reflects the
463 luminosity of the flame and MATLAB[®] recognized this reflection as part of the flame,
464 affecting, thus, a proper binarization of the flame. This reflection problem was mostly solved
465 by cropping the image before binarization to a size where the actual maximal flame could be
466 recognized reducing the reflection to a minimum. Unfortunately, the luminosity of the room
467 where the flames were recorded, was not constant. The changes of the luminosity can affect
468 the reading of the flame in the image, which could lead to wrong calculus. Therefore, five
469 different versions of the code were done, in which the binarization section of each code was
470 programmed more specific to obtain a better lecture of the flame.

471 Despite all, the true reason of the flame volume differences between Palacio's method and
472 the proposed method is unknown, the previously explained factors may affect the final
473 calculate flame volume value.

474

475 *4.2 Image processing speed*

476 Finally, one of the most remarkable advantages of the new method is the time required to
477 obtain and analyse the properties of the jet fire. The times utilized by Palacios (2017) and
478 Garcia (2019) were compared against the time used by this method.

479 The speed is represented in number of images processed per second (image/sec). That, with
480 the intention of contrast the capability of frame treatment from both methodologies, Table 5.

481

Table 5. Average processing time.

	Image set	Proposed Method [Image / s]	Regression Method [Image / s]
	7 L/min	5.3	-
	8 L/min	5.5	-
	9 L/min	5.3	-
Average	10 L/min	5.4	-
Image	0.7 atm	4.9	-
Processing	0.8 atm	5.6	-
	0.9 atm	11.9	-
	1 atm	5.6	-
	General	6.2	3.74×10^{-5}

482

483 According to Garcia (2019), his method and processing speed for P flames was three years,
484 which is 3.74×10^{-5} image per second, while the one proposed, for analyzing the same images,
485 was 6.8 image per second, which represents a huge productivity increment. Moreover, the
486 average image processing of Palacios (2017) was three years too, and the average image
487 processing speed of the MATLAB[®] code is 5.4 image per second. Generally, the new method
488 has a 6.2 image per second speed which clearly can be interpreted as fast.

489

490 Even though, the time given by Palacios and Garcia (3 years each) is not the exact time
491 expended computing the images. These 3 years represent the time expended on manually
492 computing each image of P flames or V flames and capturing the properties of the flame.
493 Also, it involves the time required to input the data in Excel[®], making graphs and obtaining
494 the regression equation, integrating that equation, and then calculating the volume, all that

495 for each image. Moreover, it could take more time if it were required the same accuracy,
496 which is not the case, as discussed before (Section 4.1).

497 While the Garcia (2019) and Palacios (2017) methods required a huge amount of human
498 effort, the one proposed was made based on computational work. Despite needing human
499 effort for developing the code, the time used (120 hours) can be neglected compared to the
500 number of images that can be processed.

501 One of the important aspects on the speed processing is the number of images per second (6
502 images), which connotes it achieved a speed fast enough to measure a proper behavior of
503 the jet fire. Nevertheless, the speed processing may be faster if the Matlab® code is more
504 optimize in order to consume less computational work or if the compute hardware
505 specifications are upgraded, because the CPU, the graphic memory, and the RAM memory
506 influence on the computational work efficiency, in this work an Intel Core 5-9400F CPU, a
507 GeForce GTX 1650 graphic card and 16 Gb of RAM are used.

508 However, being able to properly measure the behavior of a jet fire in a short period of time
509 is important, the true impact of this method on the chemical industry relies on fire safety
510 procedures, because if we are able to predict jet fire properties at different conditions, then
511 we could be able to dimension undesired but probably jet fire accidents which could be
512 mitigated by accurately plant design, on the other hand due to the processing speed, this
513 method could be implemented in the chemical industry, for example the petrochemical
514 sector, as a flame control indicator in which the jet fire properties could be specified for the
515 desire process conditions and alarm the employees if the jet fire properties are off desired jet
516 fire properties range.

517 **5. Conclusions**

518 The proposed method shows low flame lecture stability values due to a precise flame
519 analysis, meaning that the computer analysis is constant and accurate for the lecture and
520 calculus of methane flame properties. The method is an efficient alternative for the study of
521 flames, also it is very flexible and editable for the application of new geometrical
522 /mathematical models. The proposed method represents a next step in the flames research
523 because of the amount of data that can be processed. It could be beneficial in terms of time
524 and could accelerate the study of jet fires. At the end of this work, it has been possible to read
525 and analyse around 6000 flame images in 17 minutes.

526 The flame lecture stability for the proposed method was 14.61%, for Garcia (2019) method
527 was 18.64%, and for Palacios (2017) method was 75.35%, which means that the most stable
528 lecture was the proposed method. The average image processing speed of Garcia (2019) and
529 Palacios (2017) method was 3.74×10^{-5} images per second and for the proposed method was
530 6.2 image per second.

531 5.1 P flames analysis

532 The results for the average volume and width of P flames presented a decreasing pattern at
533 the evaluated sub-atmospheric pressures, but this pattern was broken at atmospheric pressure.
534 The lift off of the flame decreased and become zero once the atmospheric pressure was
535 reached, and the height of the flame showed an irregular behaviour. The comparison analysis
536 of the P flames properties (v_f , w_f , h_f , s) between the proposed method and Garcia's results had
537 very similar patterns each other. Nonetheless, the height analysis at Garcia's results
538 suggested a decreasing curve which maximum was at 0.9 atm and the proposed method
539 results suggested an irregular behaviour. Even though the results were not the same, they
540 were in a certain range of similarity. Hence, it was concluded that difference happened
541 because of each method nature.

542 5.2 V flames analysis

543 The results for the V flames volume showed an increasing pattern along with the increment
544 of methane volumetric flow, the lift off showed an increasing curve with a minimum at 8
545 L/min. Nevertheless, the comparison analysis of the V flames between the proposed method
546 and Palacios (2017) showed that they were not similar at the flame volume analysis but at
547 the lift off, width and height flame properties, a similarity could be seen. Both methods have
548 read the same flames and had relative similar values between each other, but due to the three
549 factors discussed (flame lecture stability, P2M parameter, and absolute volume values) the
550 flame volume discrepancy existed.

551 It was observed that Palacios (2017) results suggested a decreasing behaviour pattern along
552 with the volumetric flow increasing and the proposed method results suggested an increasing
553 behaviour pattern in all the geometric models. Additionally, the proposed method results
554 were compared against literature values and it was resolved that there was a close similarity.

555 However, it was determined that the main reason of the flame volume values discrepancies
556 between both methods remains unknown.

557 5.3 Future work

558 The proposed method along with the proposed geometric flame approach represents an
559 accurate, efficient, and quick tool for flames studies due to its programmable nature, the
560 image processing speed will help reduce the physical flame properties calculation and the
561 optimizing binarization parameters will help to analyse the flame lecture stability accuracy.
562 However, this method could be improved by performing the experiments in a dark
563 environment and keeping a stable camara angle along all the experiments which will benefit
564 the P2M factor calculation and therefore more accurate flame results could be obtained.

565 All the mentioned above will contribute to the flame knowledge and research. It is aware that
566 a future improvement could be optimizing the code to performed live-flame calculations,
567 which could help the chemical industry such as petrochemical, thermoelectric plants, among
568 others, to monitor flame properties at real time and leading them to take better decisions
569 regarding safety or operational issues. Although, a basic camera normally can capture
570 between 16 to 32 frames per second, pointing out that the actual process speed (6.2) is not
571 far from reaching a capability to treat fires in a *quasi-real* time, granting possibility to
572 develop tools for provide better control in the future industry.

573

574 **Acknowledgements**

575 We would like to thank the Universidad de las Americas Puebla and the Taboada Foundation
576 for the scholarships that allowed us to continue learning and enhancing our knowledge for
577 the development of science.

578 To Dr. Adriana Palacios, the supervisor of this work, for her excellent guidance and
579 knowledge contributed.

580 To Dr. Jose Luis Vazquez, scholastic from the Universidad de las Americas Puebla, for his
581 support and knowledge contribution for the development of the code and method.

582 To our parents, who have been the maximum support for us.

583 To our close friends that have been supportive, giving ideas or being good company while
584 developing the work.

585 To Erin Lescale, for reminding me what hope looks like, thank you.

586 **Nomenclature**

587	a_e	ellipsoid radius on the x-axis (m)
588	A_e	ellipse area (m ²)
589	A_f	flame vertical area (m ²)
590	b	constant in Eq. (2)
591	b_e	ellipsoid radius on the y-axis (m)
592	c_e	ellipsoid radius on the z-axis (m)
593	f_s	flame lecture stability
594	h_f	flame height (m)
595	s	flame lift off length (m)
596	$P2M$	pixel to meter ratio
597	V	flame volume
598	\bar{V}	flame volume average
599	V_e	ellipse volume
600	V_f	flame volume obtained by proposed method (m ³)
601	$V_{f, Palacios}$	flame volume obtained by Palacios method (m ³)
602	$V_{f, Ellipse}$	flame volume obtained by Baron method (m ³)
603	$V_{f, Orloff}$	flame volume obtained by Orloff method (m ³)
604	$V_{f, Garcia}$	flame volume obtained by Garcia method (m ³)
605	$V_{f, Kite}$	flame volume obtained by Zhou method (m ³)
606	w_f	flame width (m)
607	<i>Greek symbols</i>	
608	α	length ratio of lower flame to whole flame (non-dimensional)
609		
610		

611 **References**

- 612 1. Ag2gaeh. (2015, May 6). *Spheroid with coordinate axes* [Graph]. Wikipedia.
613 <https://commons.wikimedia.org/wiki/File:Ellipsoid-rot-ax.svg#/med>
- 614 2. American Institute of Chemical Engineers (AIChE). (2016). *Dow's Fire and*
615 *Explosion Index Hazard Classification Guide* (7th Revised ed.). Wiley-Aiche.
- 616 3. Annushkin, Y. M., & Sverdlov, E. D. (1978). *Stability of submerged diffusion flames*
617 *in subsonic and underexpanded supersonic gas-fuel streams. Combustion, Explosion*
618 *and Shock Waves*, 14(5), 597-605.
- 619 4. Baron, T. (1954). *Reactions in turbulent free jets-the turbulent diffusion*
620 *flame. Chemical Engineering Progress*, 50(2), 73-76.
- 621 5. Becker, H. A., & Liang, D. (1978). Visible length of vertical free turbulent diffusion
622 flames. *Combustion and Flame*, 32, 115-137.
- 623 6. Casal, J. (2017). Evaluation of the effects and consequences of major accidents in
624 industrial plants. Elsevier.
- 625 7. Castro, U. R., (2017, December). *Estudio y modelación matemática de dardos de*
626 *fuego en presiones atmosférica y subatmosférica* (TFG). Universidad de las Americas
627 Puebla. http://catarina.udlap.mx/u_dl_a/tales/documentos/lin/castro_martinez_ur/
- 628 8. Chamberlain, G. (1987). *Developments in design methods for predicting thermal*
629 *radiation from flares. Chemical Engineering Research and Design*, 65(4), 299-309.
- 630 9. Dietrich D. L., Ross H. D., Frate D. T., T'ien J. S., Shu Y. *Candle flames in*
631 *microgravity // The 3rd Int. Microgravity Combustion Workshop, NASA Lewis*
632 *Research Center, US, Cleveland, Ohio, April 11–13, 1995. — P. 31–36. —*
633 <https://ntrs.nasa.gov/search.jsp R=19960008386>.
- 634 10. Dietrich, D. L., Ross, H. D., Shu, Y., Chang, P., and T'ien, J. S. (2000), *Candle flames*
635 *in non-buoyant atmospheres. Combustion Science and Technology*, 156:1-24.
- 636 11. Ekoto, I.W., A.J. Ruggles, L.W. Creitz, J.X. Li. *Updated jet flame radiation modeling*
637 *with buoyancy corrections. Int. J. Hydrogen Energy* 39 (2014) 20570–20577.
- 638 12. Garcia, J. (2019). *Mathematical model of methane jet diffusion flames in sub-*
639 *atmospheric and atmospheric pressures* (Licenciatura). Universidad de las Américas
640 Puebla.

- 641 13. Hankinson G., B.J. Lowesmith. *A consideration of methods of determining the*
642 *radiative characteristics of jet fires*. Combust. Flame 159(2012) 1165–1177.
- 643 14. Hemmatian, B., Planas, E., & Casal, J. (2015). *Fire as a primary event of accident*
644 *domino sequences: the case of BLEVE*. *Reliability Engineering & System Safety*, 139,
645 141-148.
- 646 15. Hottel, H. C., & Hawthorne, W. R. (1948, January). *Diffusion in laminar flame jets*.
647 *In Symposium on Combustion and Flame, and Explosion Phenomena* (Vol. 3, No. 1,
648 pp. 254-266). Elsevier.
- 649 16. Hurley, M. J., Gottuk, D. T., Hall, J. R., Harada, K., Kuligowski, E. D., Puchovsky,
650 M., Torero, J. L., Watts, J. M., & Wieczorek, C. J. (2015). *SFPE Handbook of Fire*
651 *Protection Engineering*. Springer Publishing.
- 652 17. J.H. Frank, R.S. Barlow, C. Lundquist. *Radiation and nitric oxide formation in*
653 *turbulent non-premixed jet flames*. Proceedings of the Combustion Institute, Volume
654 28, Issue 1, 2000, Pages 447-454, ISSN 1540-7489, [https://doi.org/10.1016/S0082-](https://doi.org/10.1016/S0082-0784(00)80242-8)
655 [0784\(00\)80242-8](https://doi.org/10.1016/S0082-0784(00)80242-8).
- 656 18. Kalaghatigi, G. (1984). *Lift off heights and visible lengths of vertical turbulent jet*
657 *diffusion flames in still air*. Combustion Science and Technology, 41, 17.
- 658 19. Lowesmith B.J., G. Hankinson, M.R. Acton, G. Chamberlain. *An overview of the*
659 *nature of hydrocarbon jet fire hazards in the oil and gas industry and a simplified*
660 *approach to assessing the hazards*. Process. Safety Environ. 85 (2007) 207–220.
- 661 20. McDermott, R., McGrattan, K., & Hostikka, S. (2008). *Fire dynamics simulator*
662 *(version 5) technical reference guide*. NIST Special Publication, 1018, 5.
- 663 21. Orloff, L. (1981, January). *Simplified radiation modeling of pool fires*. In *Symposium*
664 *(International) on Combustion* (Vol. 18, No. 1, pp. 549-561). Elsevier.
- 665 22. Palacios, A., & Casal, J. (2011). Assessment of the shape of vertical jet
666 fires. *Fuel*, 90(2), 824-833.
- 667 23. Palacios, A., Chama, L., Villar, C. (2017). *Dardos de Fuego: Estudio Experimental*
668 *y Matemático*. XXXVIII Encuentro Nacional de la AMIDIQ. Oral Presentation. 09-
669 12 May, Guerrero, Mexico.
- 670 24. Palacios, A., M. Muñoz, R.M. Darbra, J. Casal. *Thermal radiation from vertical jet*
671 *fires*. Fire Safety J. 51 (2012) 93–101.

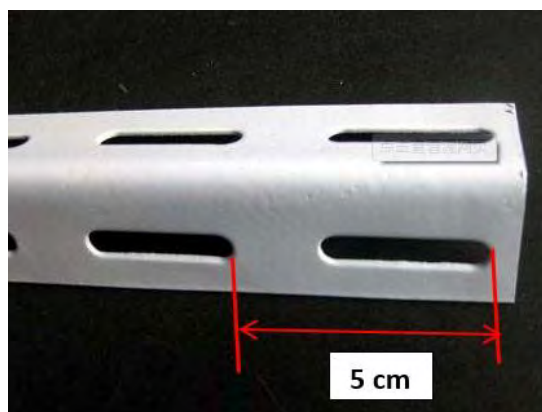
- 672 25. Parámo, A. (2019). Así fue la explosión de San Juanico. Disponible en:
673 [https://www.excelsior.com.mx/comunidad/asi-fue-la-explosion-de-san-](https://www.excelsior.com.mx/comunidad/asi-fue-la-explosion-de-san-juanico/1348517)
674 [juanico/1348517](https://www.excelsior.com.mx/comunidad/asi-fue-la-explosion-de-san-juanico/1348517). Accesado: 15 mayo 2020.
- 675 26. Schefer, R.W., Kulatilaka, W.D., Patterson, B.D., Settersten, T.B. *Visible emission of*
676 *hydrogen flames*, Combust. Flame, Bd. 156, S.1234–1241, 2009.
- 677 27. Shen, L., Zhu, D., Nadeem, S., Wang, Z., & Kaufman, A. E. (2017). *Radiative*
678 *transport based flame volume reconstruction from videos*. IEEE transactions on
679 visualization and computer graphics, 24(7), 2209-2222.
- 680 28. Sunderland, P.B., Mendelsen, B.J., Yuan, Z.–G., Urban, D.L.: *Shapes of buoyant and*
681 *nonbuoyant laminar jet diffusion flames*. Combust. Flame 116, 376 (1999)
- 682 29. UDLAP, USTC, The Royal Society. (2014). *Research project funded by The Royal*
683 *Society, Newton International Fellowship Alumni (ID: AL140028\1)*.
- 684 30. Wohl, K., & Gazley, C. (1948, January). Diffusion flames. In *Symposium on*
685 *Combustion and Flame, and Explosion Phenomena* (Vol. 3, No. 1, pp. 288-300).
686 Elsevier.
- 687 31. Zhang Y., Kim M., Guo H., Sunderland P. B., Quintiere J. G., de Ris J., Stocker D.
688 P. *Emulation of condensed fuel flames with gases in microgravity* // Combust. Flame.
689 —2015b. — V.162, N 10. — P. 3449–3455. —
690 <https://doi.org/10.1016/j.combustflame.2015.05.005>.
- 691 32. Zhang, X., Hu, L., Wang, Q., Zhang, X., & Gao, P. (2015a). *A mathematical model*
692 *for flame volume estimation based on flame height of turbulent gaseous fuel*
693 *jet*. Energy Conversion and Management, 103, 276-283.
- 694 33. Zhou, K., J. Jiang. *Thermal radiation from vertical turbulent jet flame: line source*
695 *model*. J. Heat Transfer 138 (2015) 042701.
- 696 34. Zhou, K., Liu, J., & Jiang, J. (2016). *Prediction of radiant heat flux from horizontal*
697 *propane jet fire*. Applied Thermal Engineering, 106, 634-639.
- 698 35. Zwillinger, D. (Ed.). (2011). *CRC Standard Mathematical Tables and Formulae*
699 (32nd ed.). CRC Press. <https://doi.org/10.1201/b10980>
- 700 36. Кузнецов, Е. А., Снегирёв, А. Ю., & Маркус, Е. С. (2020). *Радиационное*
701 *Погасание Ламинарного Диффузионного Пламени Над Плоской Пористой*
702 *Горелкой В Условиях Невесомости. Численное Моделирование. Физика*
703 *Горения и Взрыва*, 4, 26–45.

704

705

706 **Annex A**

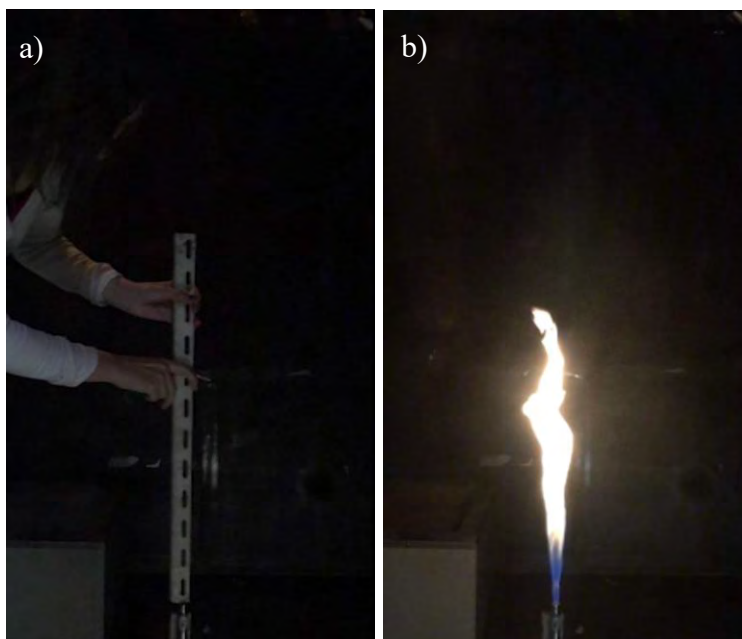
707 For the pixel to meter ratio used (P2M), it was used a metal bar already measure in centimetre
708 units. Figure 15 represents the bar used; it is shown the equivalent in centimetres to the
709 indicated section of the bar. In figure 16, it can be appreciated that a photo of the metal bar
710 was taken, to measure the ratio between pixel and meters. MATLAB[®] is able to count the
711 number of pixels that are equivalent to the 5 cm of the metal bar.



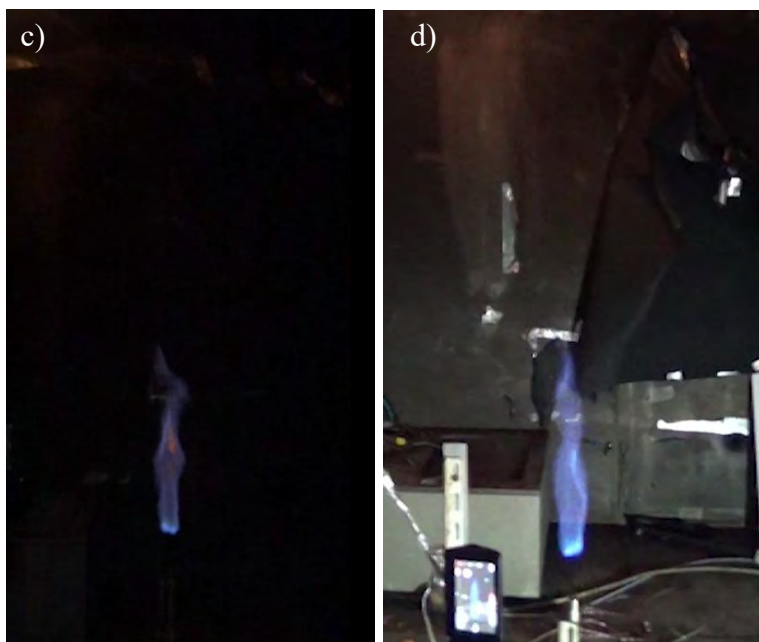
712

713

Figure 15: Metal bar size. (UDLAP *et al*, 2014)



714



715

716 Figure 16: a) Metal bar in experiment room b) 1 atm pressure Jet fire photo c) 10 L/min methane jet fire photo
717 d) 9L L/min jet fire photo. (UDLAP *et al*, 2014)

718 As it can be seen, there are different photos taken in different angles. That was a problem to
719 obtain a proper P2M ratio. The directly P2M ratio obtained was for P flames, Figure 15b, due
720 to the image has the same angle as Figure 15a. For the other photos changed of angle, Figure
721 15c and 15d, it was correlated a P2M according to some structures in the images. However,
722 the P2M for Figure 15c, was the hardest and possibly the least accurate. Luckily, Figure 15c
723 just represents the 10 L/min methane flame images.

724 Anyway, the experiments were not based or planned to execute this method proposed. For
725 further experiments, it is recommended to don't change the camera angle or zoom and have
726 a homogeneous color background.

727

728

729

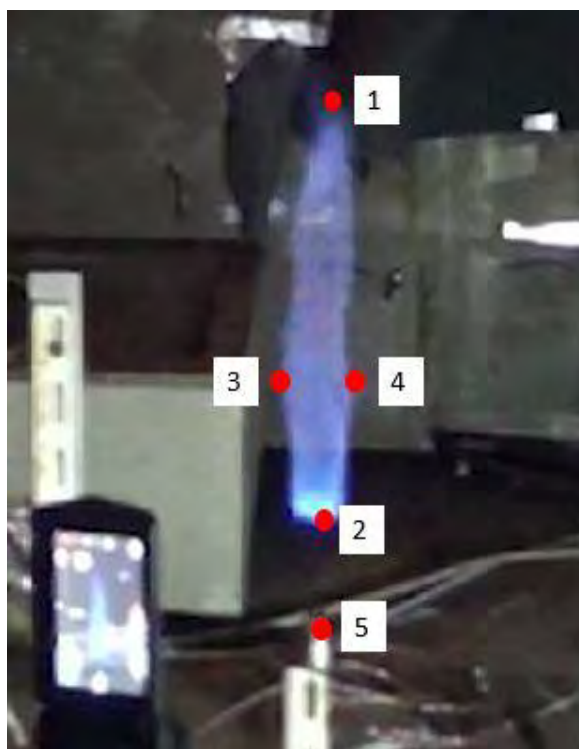
730

731

732 **Annex B**

733 For the obtention of the flame properties with MATLAB[®], the image is read, and the jet fire
734 is filtered, as already explained (Section 3.1). Parting from a localized flame, the code obtains
735 some coordinates, Figure 9, and measure the distance between them.

736 In Figure 17, it can be appreciated 5 points. Point 1, is the highest point along the z axis,
737 representing the peak of the jet fire. Point 2 is the lowest point in the flame, representing the
738 base of the fire. The height of the flame is calculated measuring the pixel distance between
739 point 1 and 2.



740

741 Figure 17: Important coordinates of the frame. (UDLAP *et al*, 2014)

742 The pixel distance between point 3 and 4, represents the maximum diameter of the flame.
743 Because of the nature of the flame and its instability, the maximum diameter changes every
744 frame. Anyway, the code is able to read all the diameters of the flame along the z axis and
745 decide the maximum diameter of each frame.

746 Finally, the point 5, Figure 17, is situated at the nozzle and outside of the methane flow. The
747 lift off is measured with the distance between point 5 and 2, where combustion starts.